Proceedings of the
Annual Stability Conference
Structural Stability Research Council
St. Louis, Missouri, April 2-5, 2019

Flexural-torsional deformations of imperfect thin-walled columns with continuous bracing

Raymond H. Plaut[1], Cristopher D. Moen[2]

Abstract
Columns with initial crookedness and twist are analyzed. Continuous elastic restraints resist bending and twisting as the compressive load is increased. The thin-walled columns are linearly elastic and deformations are small. Numerical results are presented for three examples of pinned columns with half-sine initial imperfection shapes. The first two are singly symmetric, a Cee section and a Tee section, with torsional bracing. Flexural-torsional coupling occurs between the twist and bending in the strong direction. The third example is a doubly symmetric I section with lateral bracing on one flange. Flexural-torsional deformation involves twist and bending in the weak direction. The effects of axial load, bracing stiffness, and relative orientations of the imperfections are investigated. Also, the stiffness required to restrict the twist to be a certain proportion of the initial twist is determined, which could be useful for designing compression members connected to sheathing.

1. Introduction

Thin-walled columns with open cross sections are considered. If the centroid and shear center of the cross section do not coincide, coupled flexural-torsional buckling (FTB) may occur if the column is perfect. For perfect, doubly symmetric columns with bracing that is offset from the centroid, FTB also may occur. When these columns are imperfect due to initial displacements, flexural-torsional deformation (FTD) is exhibited when axial compression is applied.

In the present analysis, the columns are assumed to be restrained continuously along their length. (Discrete bracing is considered in a companion paper.) The bracing is assumed to be linearly elastic, with constant stiffness coefficients for twist and for bending in the two principal directions. The bracing acts on the additional displacements caused by the compressive axial load. An example of continuous bracing is sheathing attached to a flange (Lee and Miller 2001; Tian et al. 2007). Also, multiple discrete braces acting on a column are sometimes modeled by continuous bracing when analyzed (Helwig and Yura 1999; McCann et al. 2013).

[1] D. H. Pletta Professor of Engineering (Emeritus), Virginia Tech <rplaut@vt.edu>
[2] CEO and President, NBM Technologies, Inc. <cris.moen@nbmtech.com>

For perfect columns, FTB of continuously braced, thin-walled columns has been considered previously, e.g., by Timoshenko and Gere (1961), Trahair and Nethercot (1984), Trahair (1993), Helwig and Yura (1999), Lee and Miller (2001), and Tian et al. (2007). For imperfect columns, research has been lacking.

Hence, the problem considered here needs to be analyzed. It is formulated in Section 2 for the general case, and the solution procedure is described. Examples of a Cee section, a Tee section, and an I section are analyzed in Sections 3, 4, and 5, respectively, followed by concluding remarks in Section 6.

2. Formulation

The column is assumed to be uniform and linearly elastic. It has length L, cross-sectional area A, modulus of elasticity E, shear modulus G, principal moments of inertia I_x and I_y about the centroid, polar moment of inertia I_0 about the shear center, torsion constant J, and warping constant C_w.

In the cross section in Fig. 1(a) for the idealized perfect column, the centroidal coordinate axes are x (horizontal) and y (vertical). The axis along the centroids is z. The shear center is located at $(x, y) = (x_0, y_0)$. The location at which continuous restraints act is denoted N and is located at $(x, y) = (h_x, h_y)$. The line connecting the centroid C and the shear center S has angle γ with the x axis.

The initial imperfect configuration is depicted in Fig. 1(b). The initial deflections in the x and y directions are $u_0(z)$ and $v_0(z)$, respectively, and the initial twist is $\phi_0(z)$, positive as shown. The locations of the centroid and shear center are denoted C' and S', respectively. The axes (x', y') are rotated by angle ϕ_0 from the (x, y) axes (cf. Fig. 4.8 of Chen and Atsuta (1977)). The bracing has rotational stiffness k_ϕ per unit length along the z axis (into the page), and translational stiffnesses k_x and k_y per unit length resisting translation parallel to the x' and y' axes, respectively.

The deflected configuration is shown in Fig. 1(c), with the springs left out of the picture. The column is subjected to compressive axial load P directed along the centroids of the cross sections of the idealized perfect configuration. The locations of the centroid and shear center are denoted C'' and S'', respectively. Compared with the initial imperfect configuration, the additional deflections of the shear center are u and v, and the additional twist is ϕ.

The ends of the column, at $z = 0$ and $z = L$, are located at $(x, y) = (0, 0)$. They are assumed to be simple supports (pinned), free to warp and to rotate about the x and y axes, but not allowed to rotate about the z axis or to deflect in the x and y directions.

It is assumed that deformations are small, with $1 + (u_0')^2 \approx 1$, $1 + (v_0')^2 \approx 1$, $\sin\phi_0 \approx \phi_0$, $\cos\phi_0 \approx 1$, and similarly for u, v, ϕ, and $u_0 + u$, $v_0 + v$, $\phi_0 + \phi$. Therefore u_0 and u are approximately parallel to the x axis, and v_0 and v are approximately parallel to the y axis.

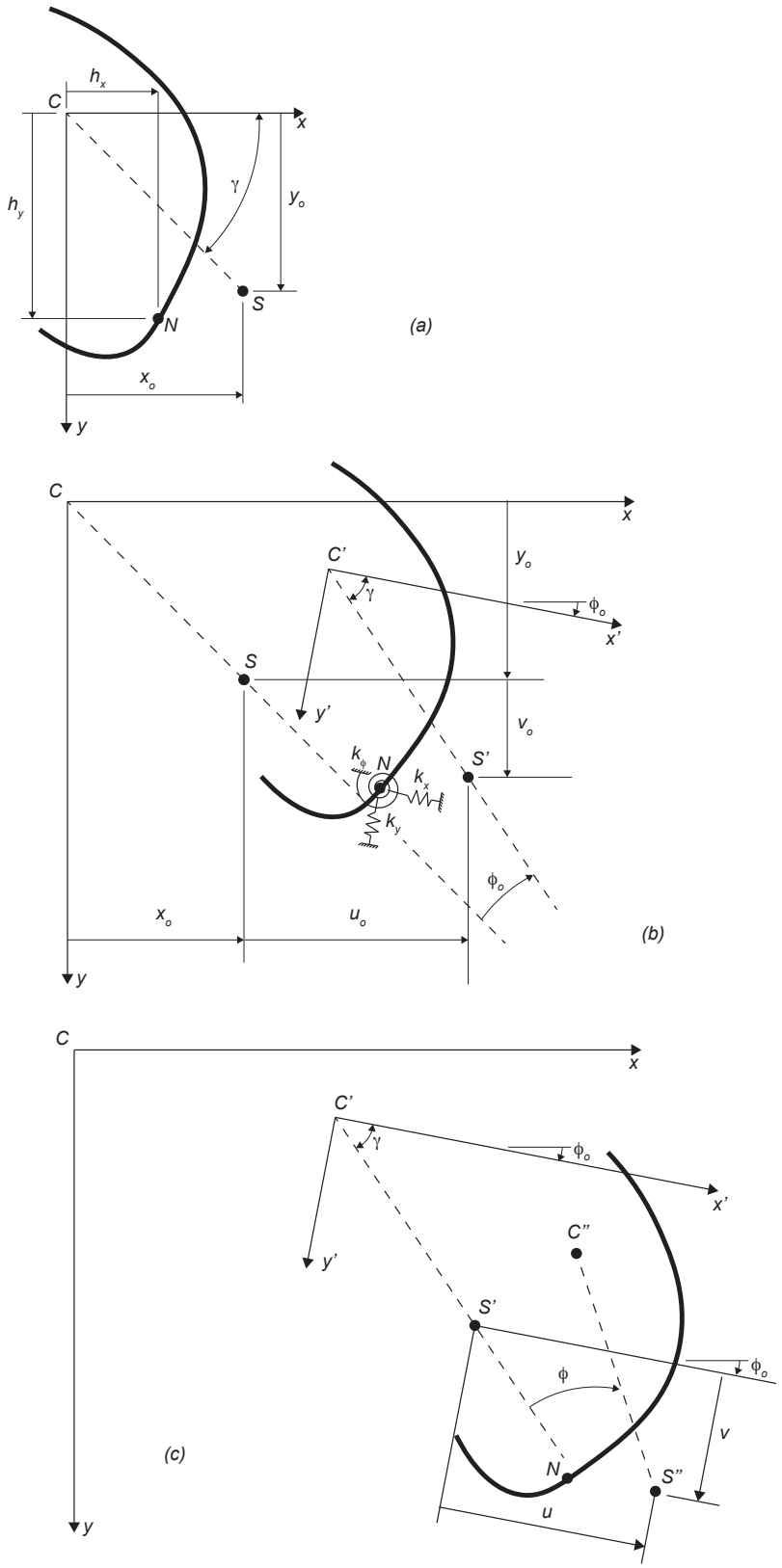

Figure 1: Geometry of cross section: (a) idealized perfect configuration; (b) initial imperfect configuration; (c) deflected configuration

The governing equilibrium equations are as follows:

$$EI_y u'''' + Pu'' + k_x u + k_x(y_0 - h_y)\phi + Py_o\phi'' = -Pu_o'' - Py_0\phi_0'', \tag{1}$$

$$EI_x v'''' + Pv'' + k_y v - k_y(x_0 - h_x)\phi - Px_o\phi'' = -Pv_o'' + Px_0\phi_0'', \tag{2}$$

$$EC_w\phi'''' - [GJ - (PI_0/A)]\phi'' + Py_0u'' + k_x(y_0 - h_y)u - Px_0v'' \\ - k_y(x_0 - h_x)v + k_x(y_0 - h_y)^2\phi + k_y(x_0 - h_x)^2\phi + k_\phi\phi = -Py_0u_0'' + Px_0v_0'' \\ - P(I_0/A)\phi_0''. \tag{3}$$

These equations were previously given in Timoshenko and Gere (1961) and Tian et al. (2007) for perfect columns (i.e., the right-hand sides were zero). The right-hand sides can be obtained from Szalai (2017) and Moen and Plaut (2018).

The initial displacements are assumed to be half-sine shapes, given by

$$u_0(z) = a_1\sin(\pi z/L), v_0(z) = a_2\sin(\pi z/L), \phi_0(z) = a_3\sin(\pi z/L). \tag{4}$$

The additional displacements due to the axial load *P* have the same form:

$$u(z) = c_1\sin(\pi z/L), v(z) = c_2\sin(\pi z/L), \phi(z) = c_3\sin(\pi z/L) \tag{5}$$

where the amplitudes c_1, c_2, and c_3 are to be determined.

Substituting Eqs. (4) and (5) into Eqs. (1)-(3), and then dividing by sin($\pi z/L$), leads to the following three algebraic equations for c_1, c_2, and c_3:

$$\alpha_{11}c_1 + \alpha_{13}c_3 = \gamma_1, \tag{6}$$
$$\alpha_{22}c_2 + \alpha_{23}c_3 = \gamma_2, \tag{7}$$
$$\alpha_{13}c_1 + \alpha_{23}c_2 + \alpha_{33}c_3 = \gamma_3, \tag{8}$$

where

$$\alpha_{11} = (\pi/L)^4EI_y - (\pi/L)^2P + k_x,\ \alpha_{13} = -(\pi/L)^2Py_0 + k_x(y_0 - h_y), \\ \alpha_{22} = (\pi/L)^4EI_x - (\pi/L)^2P + k_y,\ \alpha_{23} = (\pi/L)^2Px_0 - k_y(x_0 - h_x), \\ \alpha_{33} = (\pi/L)^4EC_w + (\pi/L)^2[GJ - (PI_0/A)] + k_x(y_0 - h_y)^2 + k_y(x_0 - h_x)^2 + k_\phi, \\ \gamma_1 = (\pi/L)^2P(a_1 + y_0a_3),\ \gamma_2 = (\pi/L)^2P(a_2 - x_0a_3), \\ \gamma_3 = (\pi/L)^2P[y_0a_1 - x_0a_2 + (I_0/A)a_3]. \tag{9}$$

For the case of a perfect column ($a_1 = a_2 = a_3 = 0$), the critical load is found by setting the determinant of the matrix of the coefficients α_{ij} equal to zero. For imperfect columns, Eqs. (6)-(8) are solved for c_1, c_2, and c_3. FTD involves twist and bending. In the examples to be considered in the following section, bending in one direction will be uncoupled, and FTD will involve twist and bending in either the strong or weak direction.

3. Example 1

The first example is a cold-formed steel stud column with singly symmetric 362S162-54 lipped Cee cross section (SSMA 2001), as shown in Fig. 2. It was analyzed in Moen and Plaut (2018) with no bracing, and approximately in Moen (2018) with a discrete torsional brace at midheight.

The column has L = 2438 mm (8 ft), A = 272 mm^2 (0.422 in.^{2}), I_x = 363,370 mm^4 (0.873 in.^{4}), I_y = 64,100 mm^4 (0.154 in.^{4}), $I_0 = I_x + I_y + (x_0^2 + y_0^2)A$ = 716,363 mm^4 (1.728 in.^{4}), J = 188 mm^4 (4.51×10^{-4} in.^{4}), C_w = 122,720,891 mm^4 (0.457 in.^{4}), E = 200 kN/mm^2 (29,000 kip/in.^{2}), and G = E/2.6. Unless otherwise stated, the amplitudes of the imperfections are $a_1 = a_2 = L/1000$ and a_3 = 0.00766 rad for this example.

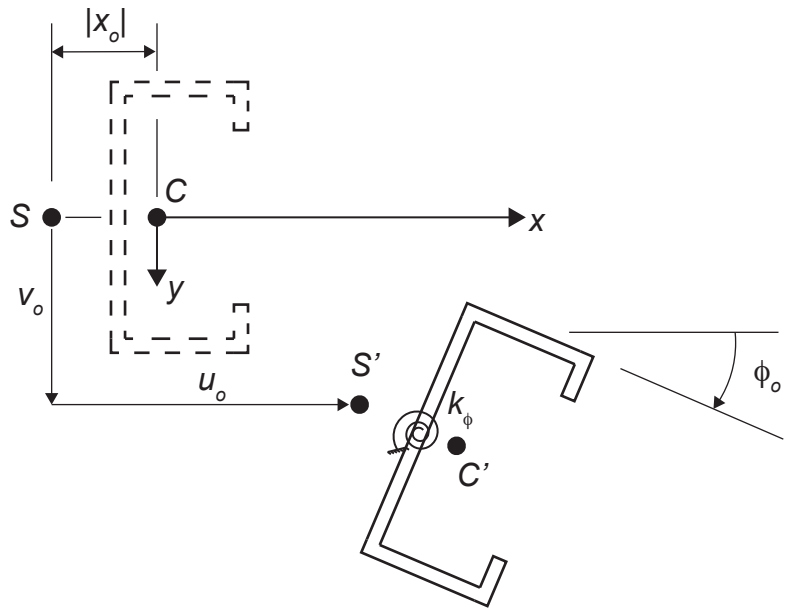

Figure 2: Example 1 cross section; idealized perfect configuration is dashed, initial imperfect configuration is solid

The overall depth of the cross section is 92.1 mm (3.625 in.), the overall width of the flanges is 41.3 mm (1.625 in.), the overall length of the lips is 12.7 mm (0.5 in.), and the thickness of the cross section is 14.4 mm (0.057 in.). The distance of the shear center to the centerline of the web is 19.7 mm (0.774 in.), x_0 = –32.59 mm (–1.283 in.), and y_0 = 0. A torsional spring with stiffness k_f acts on the cross section along the column. Its location in Fig. 2 is arbitrary.

Since $y_0 = k_y = 0$, Eq. (6) becomes uncoupled from Eqs. (7) and (8), and FTD involves twist ϕ and deflection v in the strong direction. For the idealized perfect column ($a_1 = a_2 = a_3 = 0$), the critical load for FTB is plotted versus k_ϕ in Fig. 3. It is equal to 19.5 kN when $k_\phi = 0$. The critical load for bending in the weak direction is $\pi^2 EI_y/L^2$, which is 21.3 kN. For both types of buckling, the buckling mode is given by Eq. (5), i.e., a half-sine shape (for any value of k_ϕ).

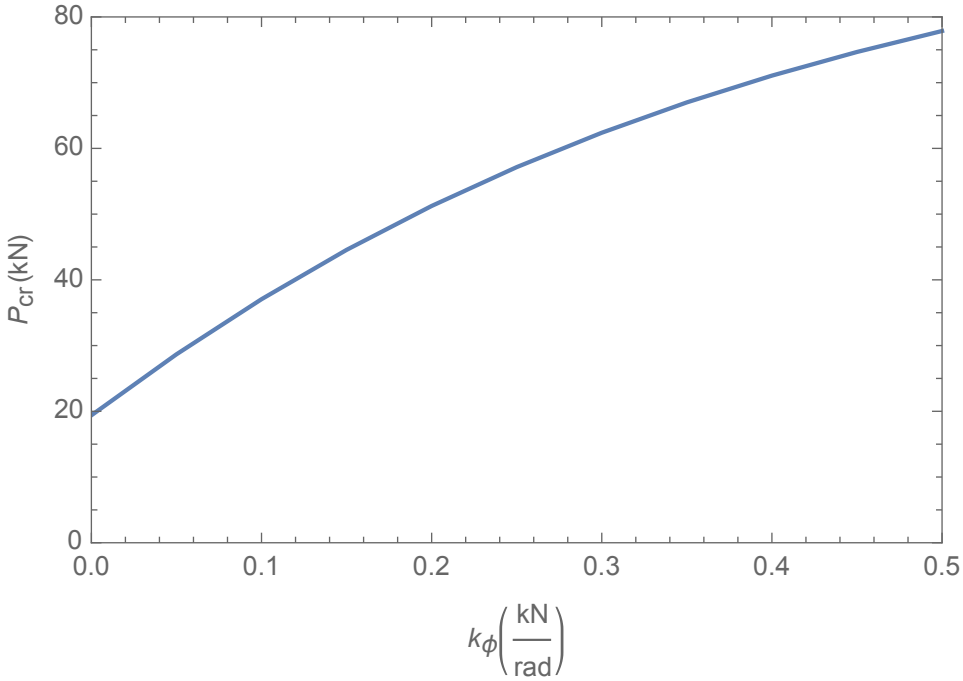

Figure 3: Flexural-torsional critical load versus k_ϕ for Example 1

For the imperfect column, Eqs. (7) and (8) are solved for c_2 and c_3. The effect of k_ϕ on the total midheight twist $a_3 + c_3$ is depicted in Fig. 4 for three loads: P = 5, 10, and 15 kN. As k_ϕ is increased from zero, initially the twist decreases sharply, and then the additional twist ϕ approaches zero. A similar behavior is observed in Fig. 5 for the coupled strong-direction midheight deflection $a_2 + c_2$.

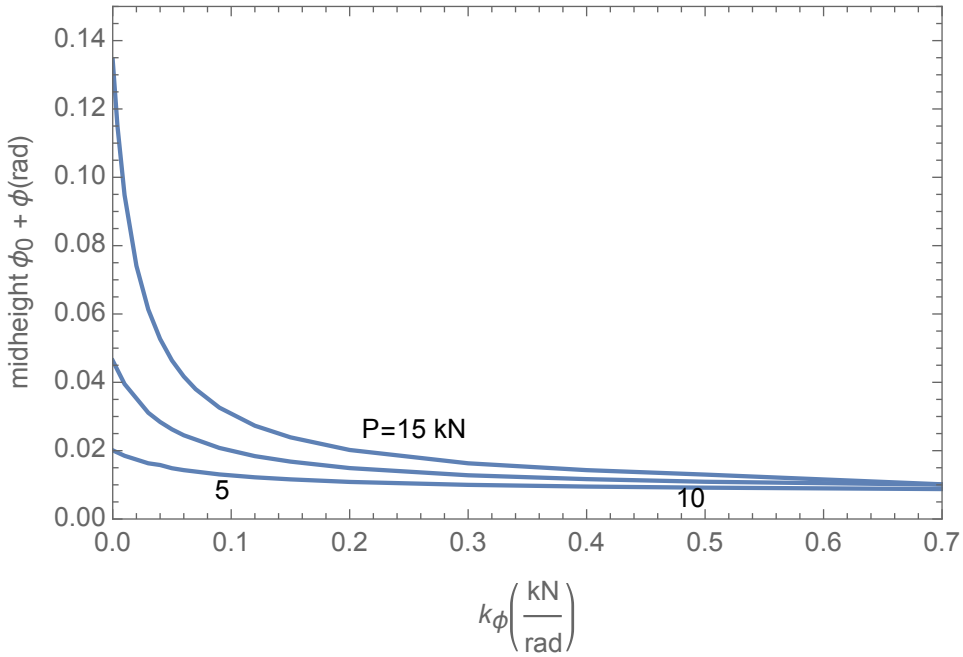

Figure 4: Total midheight twist versus k_ϕ for Example 1; P = 5, 10, 15 kN

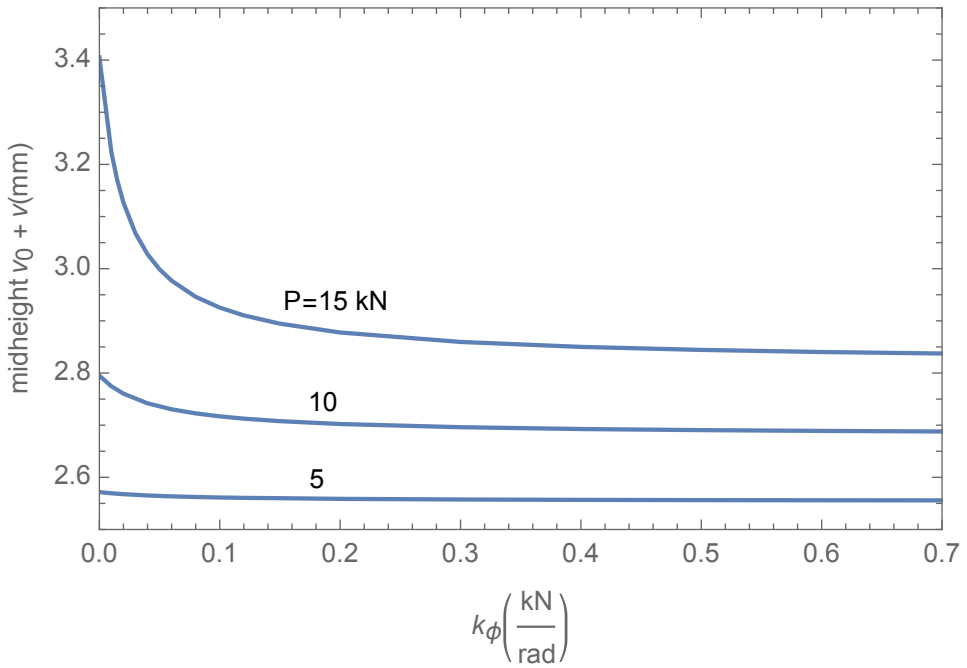

Figure 5: Total midheight deflection in strong direction versus k_ϕ for Example 1; P = 5, 10, 15 kN

If a vertical spring were included in Fig. 2 with stiffness k_y, and if k_y were increased from zero, the twist and the deflection in the strong direction would decrease.

The signs of the initial imperfections can affect the response. For the standard case, the amplitudes in Eqs. (4) are taken to be positive, with the initial deflection in the strong direction being $a_2 = L/1000 = 2.438$ mm in this example. Figs. 6 and 7 show the effects of this amplitude being zero or $-L/1000$, while the initial twist amplitude a_3 remains 0.00766 rad. The stiffness k_ϕ is fixed at 0.25 kN/rad. At a given load P, the magnitude of the twist is largest for the case $a_2 = L/1000$ (Fig. 6), whereas the magnitude of $v_0(L/2) + v(L/2)$ does not depend significantly on the sign of a_2 (Fig. 7).

If the signs of both v_0 and ϕ_0 were changed, the signs of v and ϕ would change but their magnitudes would remain the same.

Winter (1960) has suggested that torsional bracing should be sufficiently stiff so that the additional twist is not greater than the initial twist. For the standard values of a_2 and a_3, this condition is depicted by the middle curve in Fig. 8, where the load is plotted versus k_f. The lower curve gives the required stiffness for the additional twist to be half the initial twist, and the upper curve gives the required stiffness for the additional twist to be twice the initial twist. For example, if P = 10 kN, k_f must be at least 0.187 kN/rad to assure that the additional twist will not be greater than the original twist. Since the initial twist and additional twist both have half-sine forms, their ratio is the same along the column.

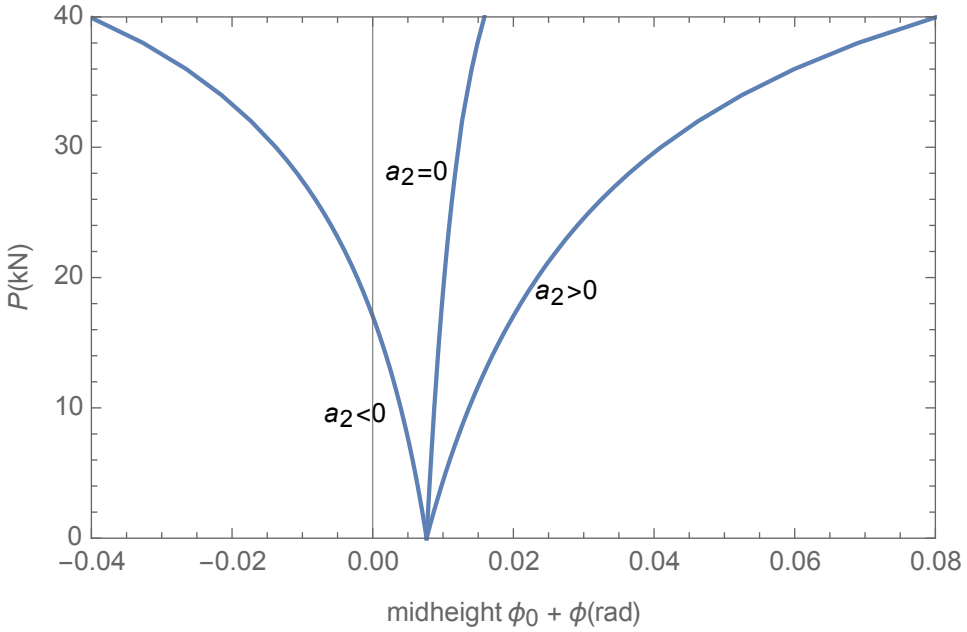

Figure 6: Load versus midheight twist for Example 1 with k_f = 0.25 kN/rad; a_2 = L/1000, 0, -L/1000

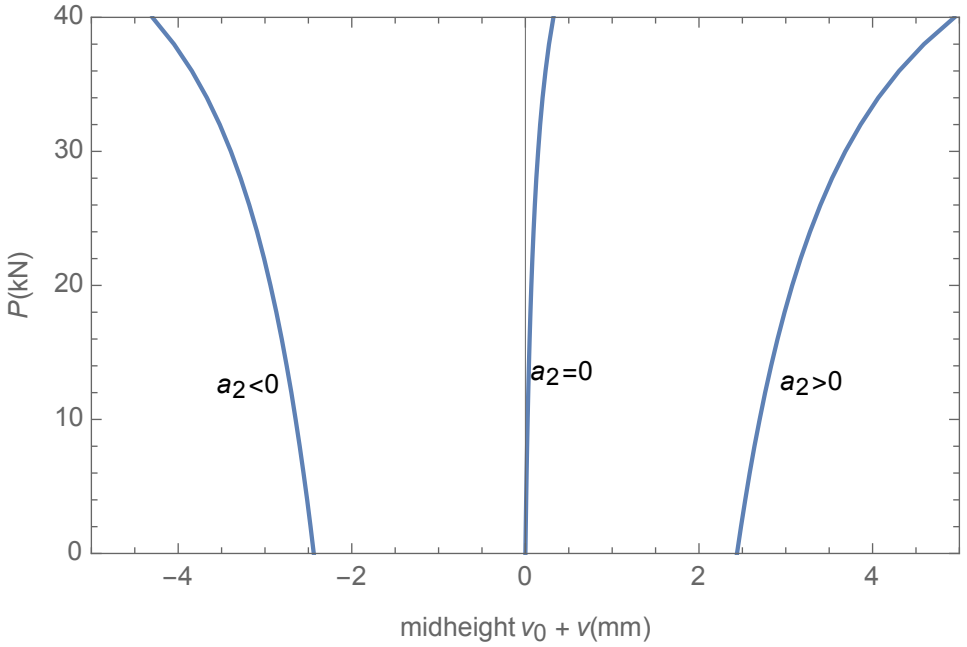

Figure 7: Load versus total midheight deflection in strong direction for Example 1 with k_f = 0.25 kN/rad; a_2 = L/1000, 0, –L/1000

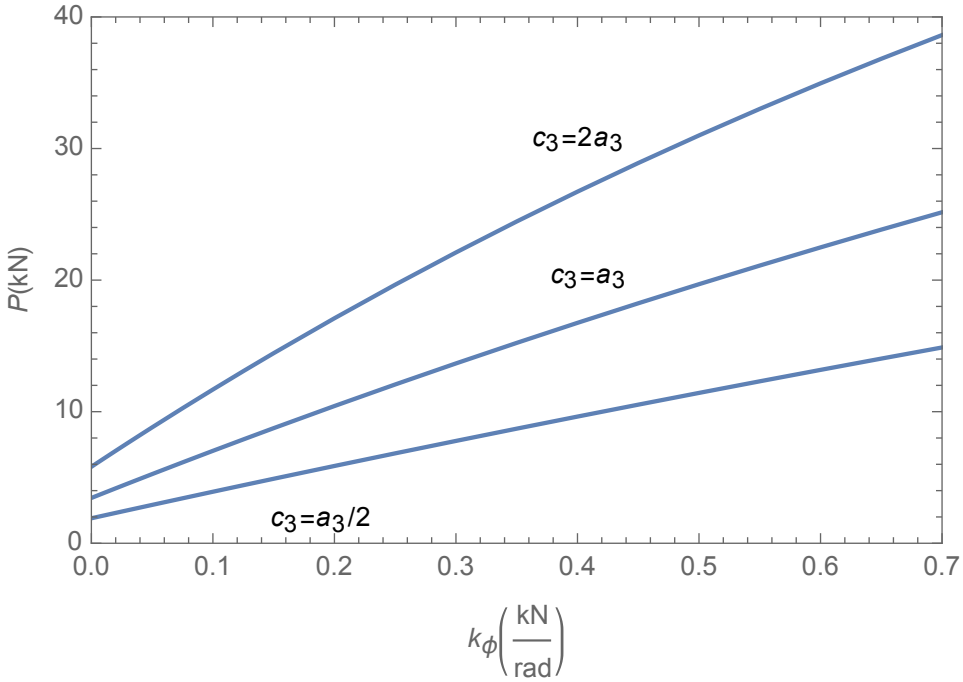

Figure 8: Load versus k_ϕ for Example 1; $c_3 = a_3/2$, a_3, $2a_3$

4. Example 2

The second example is a steel column with singly symmetric Tee cross section MT6.25×6.2 (AISC 2017), as sketched in Fig. 9. It has L = 6100 mm (20 ft), A = 6450 mm^2 (10.0 in.^{2}), I_x = 1.357×10^7 mm^4 (32.6 in.^{4}), I_y = 2.527×10^7 mm^4 (60.7 in.^{4}), I_0 = 4.17×10^7 mm^4 (100.2 in.^{4}), J = 624,350 mm^4 (1.50 in.^{4}), C_w = 8.62×10^8 mm^6 (3.21 in.^{6}), E = 200 kN/mm^2 (29,000 ksi), and G = E/2.6. Unless otherwise stated, the amplitudes of the imperfections are $a_1 = a_2 = L/1000$ and a_3 = 0.0192 rad for this example.

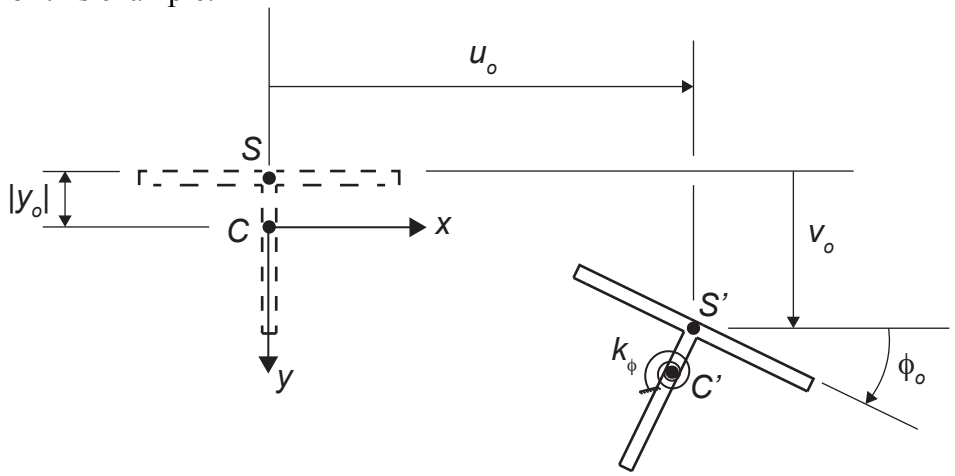

Figure 9: Example 2 cross section; idealized perfect configuration is dashed, initial imperfect configuration is solid

The overall depth of the cross section is 178 mm (7.02 in.), the width of the flange is 254 mm (10.0 in.), the thickness of the web is 10.5 mm (0.415 in.), and the thickness of the flange is 46.0 mm (1.81 in.). The shear center is at the intersection of the centerlines of the web and flange, x_0

= 0, and y_0 = –23.6 mm (–0.930 in.). A torsional spring with stiffness k_ϕ acts on the cross section along the column. Its location in Fig. 9 is arbitrary.

For this example, $x_0 = k_x = 0$ and Eq. (7) is uncoupled from Eqs. (6) and (8). Twist is again coupled with the strong-direction deflection, which now is u. The critical load for FTB of the idealized perfect column is plotted versus k_ϕ in Fig. 10. The range on the vertical axis is 1310 to 1340 kN. The critical load is equal to 1316 kN for the unbraced column ($k_\phi = 0$), whereas the critical load for bending in the weak direction is $\pi^2 EI_x/L^2 = 720$ kN. For both types of buckling, the mode is given by Eq. (5).

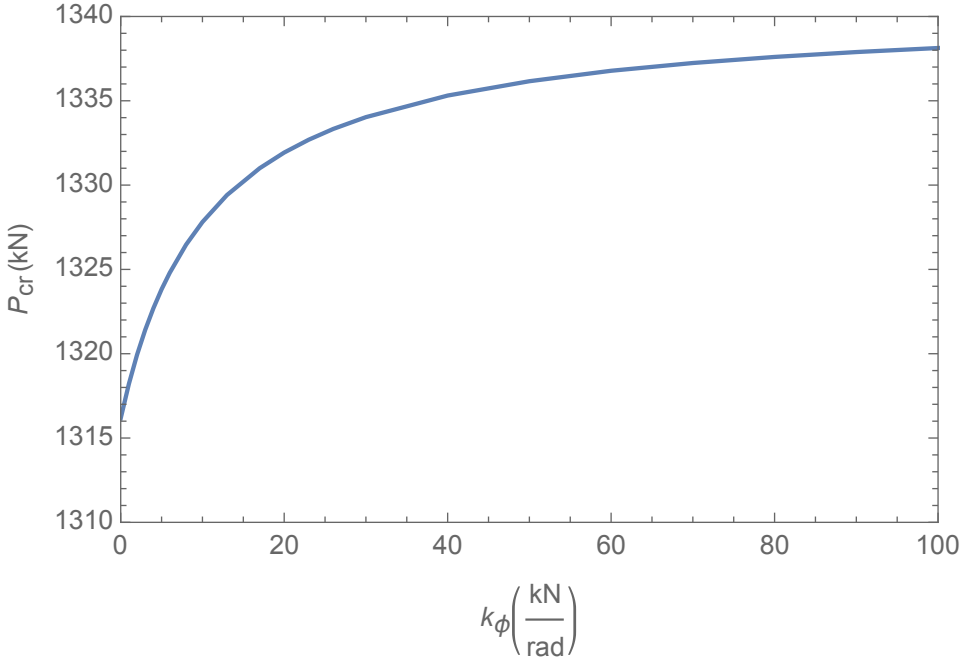

Figure 10: Flexural-torsional critical load versus k_ϕ for Example 2

For the imperfect column, the effect of k_ϕ on the twist is shown in Fig. 11 for P = 200, 400, and 600 kN. The range on the vertical axis is 0.019 to 0.025 rad. The behavior is similar to that in Fig. 4. In this example, k_ϕ has little effect on the midheight deflection in the coupled strong direction, so a graph similar to Fig. 5 is not presented. (As k_ϕ increases from 0 to 100 kN/rad, $a_2 + c_2$ decreases by 0.01%, 0.07%, and 0.28%, respectively, for P = 200, 400, and 600 kN.)

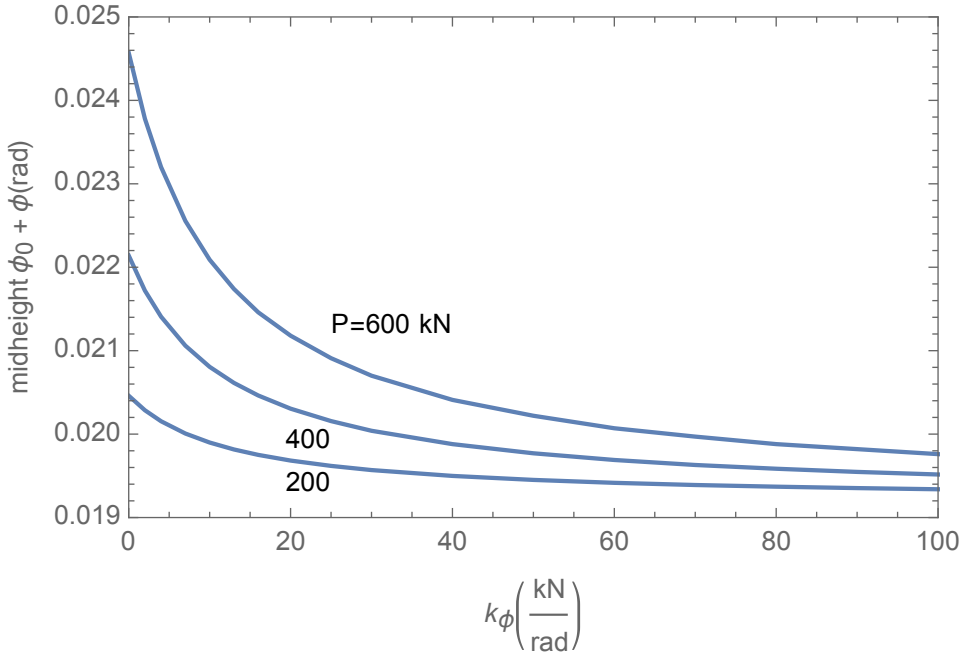

Figure 11: Total midheight twist versus k_ϕ for Example 2; P = 200, 400, 600 kN

If a lateral spring were included in Fig. 9 with stiffness k_x, and if k_x were increased from zero, the twist would tend to increase and the deflection in the strong direction would decrease.

Figs. 12 and 13 are similar in form to Figs. 6 and 7, respectively, but the right curves here are for negative initial deflection a_2 in the strong direction, and the left curves are for positive a_2. Another difference is that the twist remains positive for the range shown in Fig. 11, unlike Fig. 6.

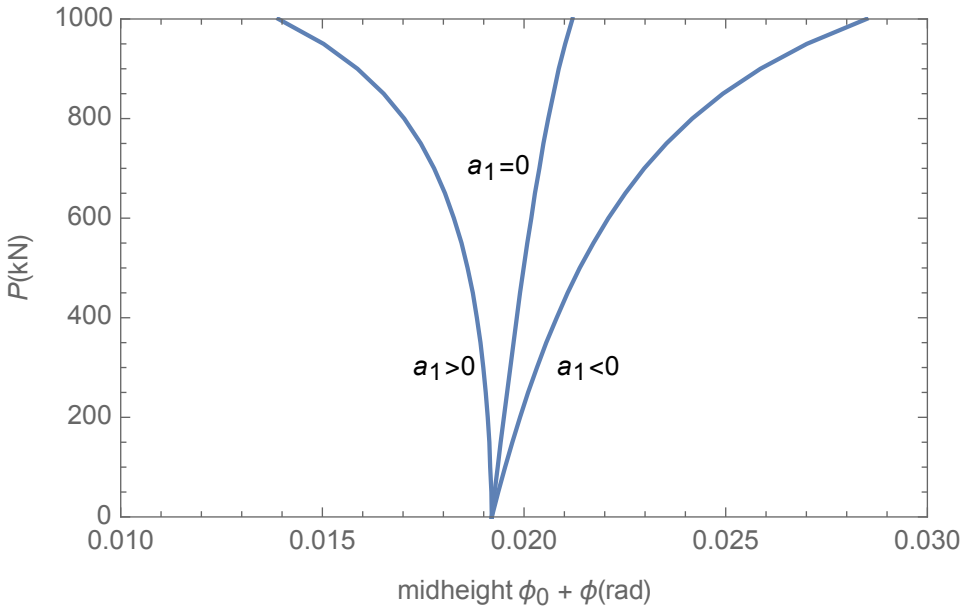

Figure 12: Load versus midheight twist for Example 2 with k_ϕ = 10 kN/rad; $a_1 = L/1000, 0, -L/1000$

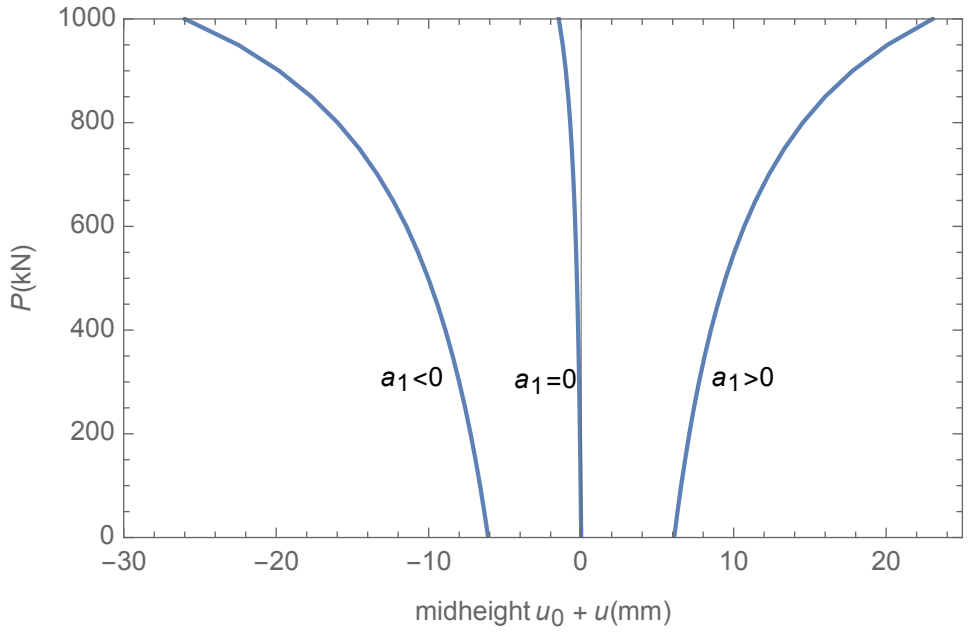

Figure 13: Load versus total midheight deflection in strong direction for Example 2 with k_ϕ = 10 kN/rad; a_1 = L/1000, 0, –L/1000

Finally, Fig. 14 is similar to Fig. 8, showing the required value of k_ϕ to restrict the additional twist to be either half, the same as, or twice the initial twist. The range on the vertical axis is 800 to 1400 kN.

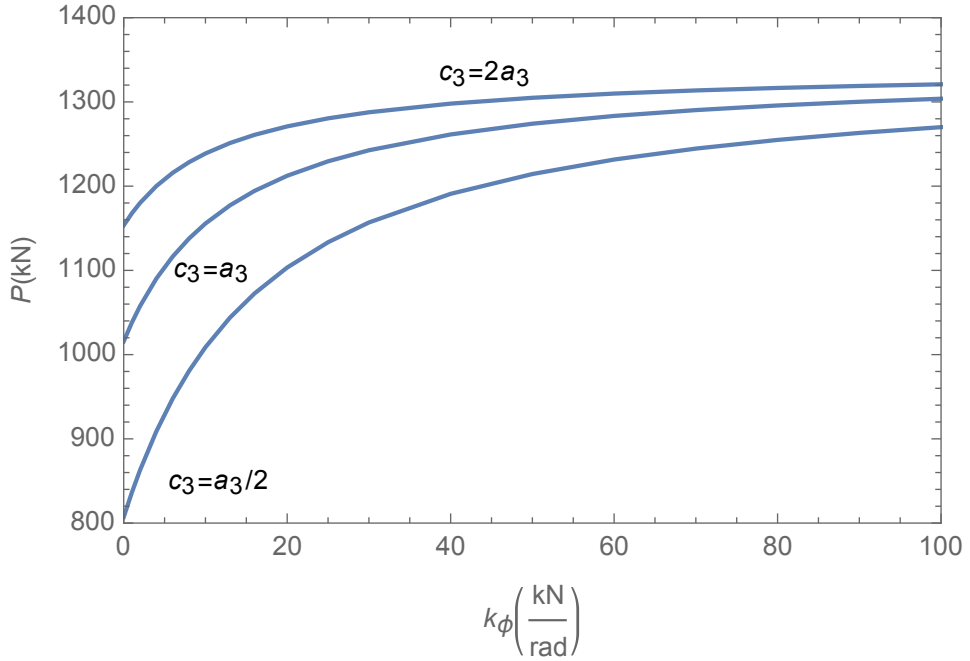

Figure 14: Load versus k_f for Example 2; c_3 = a_3/2, a_3, 2a_3

5. Example 3

The third example is a steel column with doubly symmetric I cross section W18×35 (Liu et al. 2013) and lateral bracing that is offset from the centroid (Fig. 15). The column has L = 2438 mm (8 ft), A = 6650 mm^2 (10.3 in.^{2}), $x_0 = 0$, $y_0 = 0$, $I_x = 2.12\times10^8$ mm^4 (510 in.^{4}), $I_y = 6.37\times10^6$ mm^4 (15.3 in.^{4}), $I_0 = 2.19\times10^8$ mm^4 (525 in.^{4}), $J = 2.11\times10^5$ mm^4 (0.506 in.^{4}), $C_w = 3.06\times10^{11}$ mm^6 (1140 in.^{6}), E = 200 kN/mm^2 (29,000 ksi), and $G = E/2.6$. Unless otherwise stated, the amplitudes of the imperfections are $a_1 = a_2 = L/1000$ and $a_3 = 0.00766$ rad for this example.

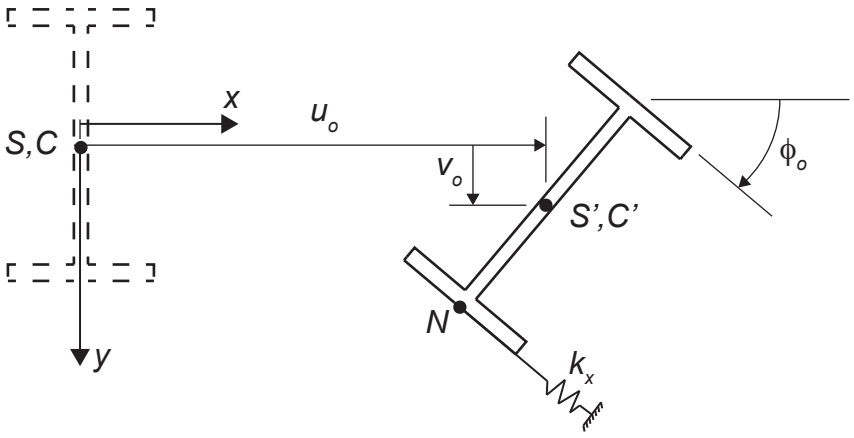

Figure 15: Example 3 cross section; idealized perfect configuration is dashed, initial imperfect configuration is solid

The overall depth of the cross section is 450 mm (17.7 in.), the width of the flanges is 152 mm (6.00 in.), the thickness of the web is 7.62 mm (0.300 in), and the thickness of the flanges is 10.8 mm (0.425 in.). A lateral spring with stiffness k_x acts at the bottom of the lower flange, attached at the centerline of the web, so that $h_x = 0$ and h_y = 225 mm (8.85 in.).

For this example, Eq. (7) is uncoupled due to $x_0 = h_x = 0$. Eqs. (6) and (8) are coupled due to k_x and h_y being nonzero, so that FTB and FTD involve twist and bending in the weak direction (unlike Examples 1 and 2). For the idealized perfect column ($a_1 = a_2 = a_3 = 0$), the critical load for FTB is plotted versus k_x in Fig. 16. The vertical axis has range 2100 to 2700 kN. The critical load is equal to 2115 kN when $k_x = 0$. The critical load for bending in the strong direction is $\pi^2 EI_x/L^2$, which is 70,400 kN. For both types of buckling, the mode is given by Eq. (5).

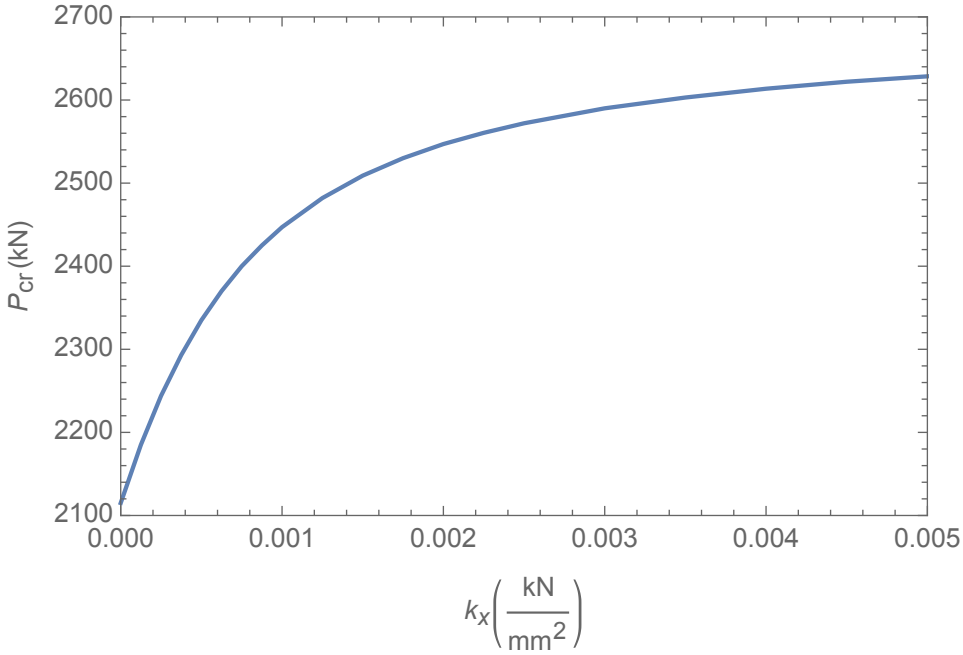

Figure 16: Flexural-torsional critical load versus k_x for Example 3

For the imperfect column, the effect of k_x on the twist is shown in Fig. 17 for P = 250, 500, and 750 kN. The range on the vertical axis is 0.008 to 0.012 rad. The behavior is opposite to that in Figs. 4 and 11, where the horizontal axis was a rotational spring stiffness rather than the stiffness of a lateral spring offset from the centroid. For a given load P, as k_x is increased, the total twist increases. In Fig. 18, the coupled deflection in the weak direction decreases with increasing bracing stiffness, as in Fig. 5. The range on the vertical axis in Fig. 18 is 2.6 to 3.8 mm.

If a rotational spring were included in Fig. 15 with stiffness k_ϕ, and if k_ϕ were increased from zero, the twist and the deflection in the weak direction would decrease.

Fig. 19 is similar to Fig. 6 except that the coupled deflection here is the deflection in the weak direction, and the twist remains positive for the range shown. The lateral spring stiffness is fixed at k_x = 0.01 kN/mm^2. The range on the horizontal axis is 0.006 to 0.013 mm. Finally, Fig. 20 is similar to Fig. 7, with a_1 replacing a_2 in Fig. 20.

No figure is presented similar to Figs. 8 and 14, since the twist does not decrease as k_x increases.

Liu et al. (2013) considered an I section with bracing similar to that in Fig. 15 but with no imperfections and with N fixed in space, so that N was the center of twist (i.e., constrained-axis FTB). The critical load for FTB for that case can be computed from the present analysis (see last paragraph of Section 2) by letting $k_x \to \infty$.

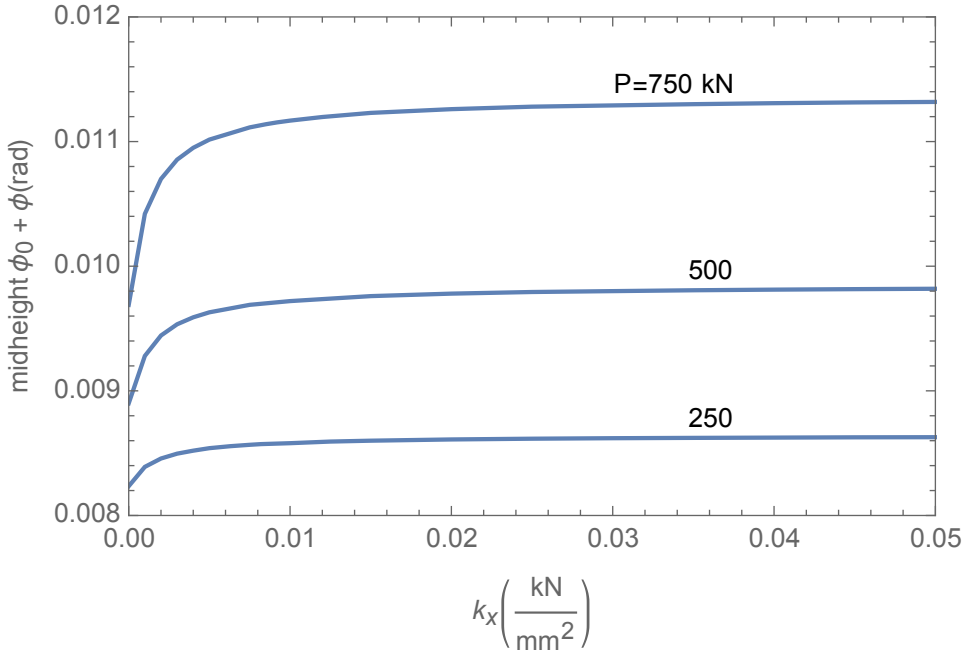

Figure 17: Total midheight twist versus k_x for Example 3; P = 250, 500, 750 kN

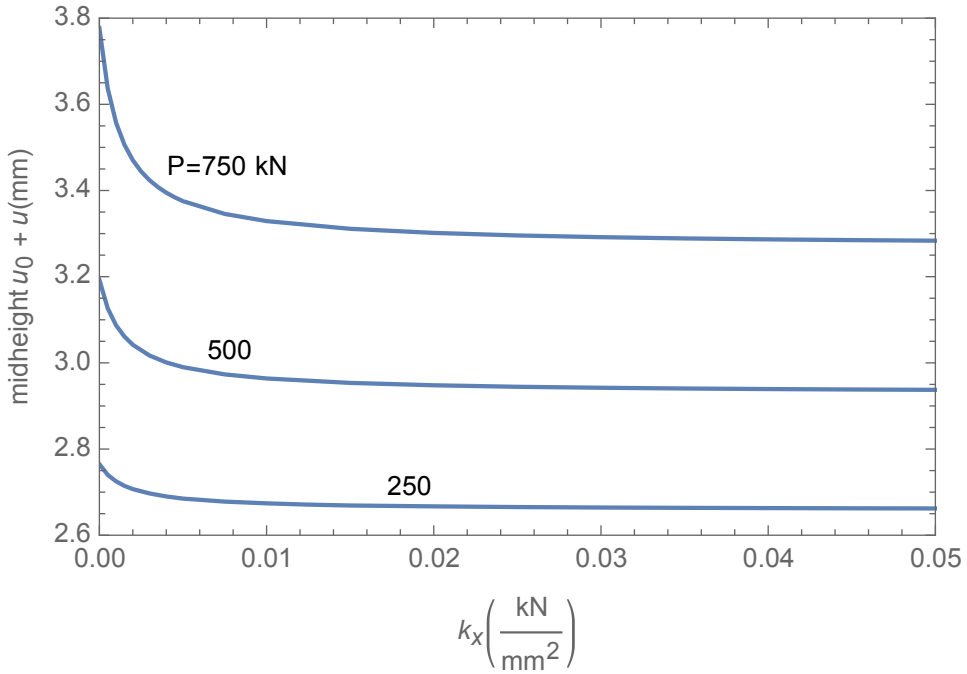

Figure 18: Total midheight deflection in weak direction versus k_x for Example 3; P = 250, 500, 750 kN

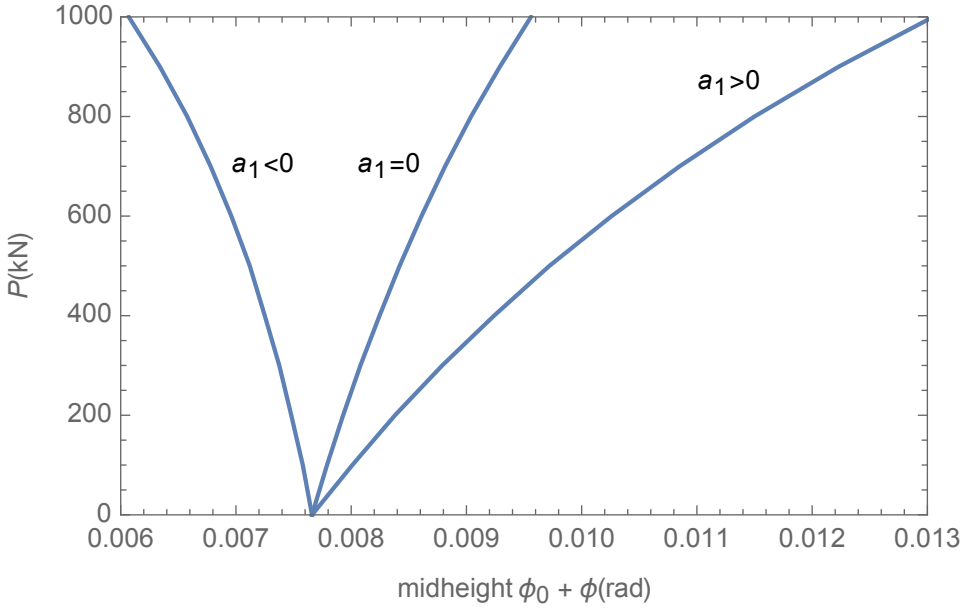

Figure 19: Load versus midheight twist for Example 3 with k_x = 0.01 kN/mm^2; a_1 = L/1000, 0, –L/1000

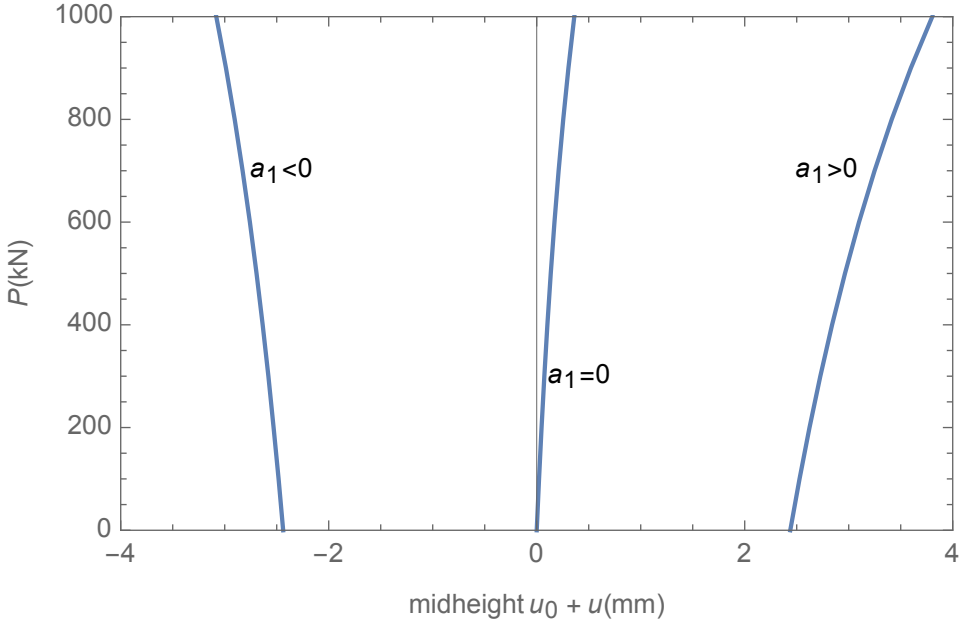

Figure 20: Load versus total midheight deflection in weak direction for Example 3 with k_x = 0.01 kN/mm^2; a_1 = L/1000, 0, –L/1000

6. Concluding Remarks

Flexural-torsional deformation (FTD) of thin-walled columns with open cross sections has been analyzed. The columns have initial deflections and/or twist, and are subjected to an axial compressive load that acts along the centroids of the cross sections of the idealized perfect column. Continuous bracing is modeled by distributions of translational and torsional springs. It is assumed that deformations are small, and that the column and restraints are linearly elastic.

It is assumed that the column ends are pinned and free to warp, and that the initial imperfections are half-sine shapes. The general equilibrium equations were presented and solved. For three examples, the effects of the bracing stiffness, senses (signs) of the imperfections, and magnitude of the compressive load were examined. Also, the required bracing stiffness for a specified restriction on the twist was determined for Examples 1 and 2. Flexural-torsional buckling (FTB) was discussed for the case of a perfect column.

A Cee section with torsional bracing was considered in Example 1. FTD involved twist and deflection in the strong direction. A Tee section with torsional bracing was studied in Example 2, and FTD again involved twist and deflection in the strong direction. In Example 3, an I section was considered, with lateral bracing acting on one flange, and FTD involved twist and deflection in the weak direction.

For perfect columns, it was stated in Gardner and Nethercot (2005) and Ziemian (2010) that FTB does not occur if the centroid and shear center coincide. However, Example 3 demonstrated that it can if there is lateral bracing that is offset from that location on the cross section.

It was found that a change in sense of the initial deflection involved in FTD, or a lack of that imperfection, can cause a significant change in the displacements under axial load.

If the initial imperfections in Eq. (4) were to contain additional functions $\sin(j\pi z/L)$ with $j > 1$, the corresponding displacements to be superposed could be obtained using Eqs. (4)-(9) with π replaced by $j\pi$.

It would not be easy to develop design formulas or charts for FTD, since many parameters are involved. In nondimensional terms, these could include I_x/I_y, I_0/I_y, $EC_w/(GJL^2)$, x_0/L, y_0/L, h_x/L, h_y/L, $PL^2/(EI_y)$, k_x/E, k_y/E, $k_\phi L^2/(EI_y)$, and the amplitudes and shapes of the initial imperfections.

References

AISC (2017). *AISC Shapes Database*, v15.0, American Institute of Steel Construction, Chicago, IL.

Chen, W. F., and Atsuta, T. (1977). *Theory of Beam-Columns*, Vol. 2, McGraw-Hill, New York.

Gardner, L., and Nethercot, D. A. (2005). *Designers' Guide to EN 1993-1-1 Eurocode 3: Design of Steel Structures*, Thomas Telford, London.

Helwig, T. A., and Yura, J. A. (1999). "Torsional bracing of columns." *Journal of Structural Engineering*, 125(5), 547-555.

Lee, Y.-K., and Miller, T. H. (2001). "Axial strength determination for gypsum-sheathed, cold-formed steel wall stud composite panels." *Journal of Structural Engineering*, 127(6), 608-615.

Liu, D., Davis, B., Arber, L., and Sabelli, R. (2013). "Torsional and constrained-axis flexural-torsional buckling tables for steel W-shapes in compression." *Engineering Journal*, 50(4), 205-247.

McCann, F., Wadee, M. A., and Gardner, L. (2013). "Lateral stability of imperfect discretely braced steel beams." *Journal of Engineering Mechanics*, 139(10), 1341-1349.

Moen, C. D. (2018). "Bracing design for torsional buckling of cold-formed steel wall stud columns." *Proceedings of the 24th International Specialty Conference on Cold-Formed Steel Structures*, St. Louis, MO, November 7-8, 2018.

Moen, C. D., and Plaut, R. H. (2018). "Calculation of twist and flexural deformations for a thin-walled column with initial imperfections." *Proceedings of the Eighth International Conference on Thin-Walled Structures - ICTWS 2018*, Lisbon, Portugal, July 24-27, 2018.

SSMA (2001). *SSMA Product Technical Information ICBO ER-4943P*, Steel Stud Manufacturers Association, Chicago, IL.

Szalai, J. (2017). "Complete generalization of the Ayrton-Perry formula for beam-column buckling problems." *Engineering Structures*, 153, 205-223.
Tian, Y. S., Wang, J., and Lu, T. J. (2007). "Axial load capacity of cold-formed steel wall stud with sheathing." *Thin-Walled Structures*, 45, 537-551.
Timoshenko, S. P., and Gere, J. M. (1961). *Theory of Elastic Stability*, 2nd edition, McGraw-Hill, New York.
Trahair, N. S. (1993). *Flexural-Torsional Buckling of Structures*, CRC Press, Boca Raton, FL.
Trahair, N. S., and Nethercot, D. A. (1984). "Bracing requirements in thin-walled structures." In: *Developments in Thin-Walled Structures - 2*, J. Rhodes and A. C. Walker, editors, Elsevier, London, 93-130.
Winter, G. (1960). "Lateral bracing of columns and beams." *Transactions of the American Society of Civil Engineers*, 125(1), 807-845.
Ziemian, R.D, editor (2010). *Guide to Stability Design Criteria for Metal Structures,* 6th edition, Wiley, New York.